Photoproduction of possible pentaquark states $\Lambda_b^0(5912)$ and $\Lambda_b^0(5920)$ in the $\gamma p \to \Lambda_b^{0(*)} B^+$ reactions

Yin Huang[1] and Hong Qiang Zhu[2,*]

[1]*School of Physical Science and Technology, Southwest Jiaotong University, Chengdu 610031, China*
[2]*College of Physics and Electronic Engineering, Chongqing Normal University, Chongqing 401331, China*

(Received 16 July 2021; accepted 9 September 2021; published 28 September 2021)

In this work, we report on a theoretical study of possible pentaquark states $\Lambda_b^0(5912)$ and $\Lambda_b^0(5920)$ in the $\gamma p \to \Lambda_b^{0(*)} B^+$ reactions within an effective Lagrangian approach. In addition to the contributions from the s-channel nucleon pole and t-channel $\bar{B}^{*-}$ exchange, the contact term contribution is also included. Our theoretical approach is based on the chiral unitary theory where the $\Lambda_b^0(5912)$ and $\Lambda_b^0(5920)$ resonances are dynamically generated. Within the coupling constants of the $\Lambda_b^0(5912)$ and $\Lambda_b^0(5920)$ to $\bar{B}p$ and $\bar{B}^* p$ channels obtained from chiral unitary theory, the total and differential cross sections of the $\gamma p \to \Lambda_b^{0(*)} B^+$ are evaluated. Our calculation indicates that the cross section for $\gamma p \to \Lambda_b^0(5912) B^+$ and $\gamma p \to \Lambda_b^0(5920) B^+$ reactions are of the order of 0.0164 and 0.00527 nb, respectively. If measured in future experiments, such as the Electron-Ion Collider in China or the United States, then the predicted total cross sections and specific features of the angular distributions can be used to test the (molecular) nature of the $\Lambda_b^0(5912)$ and $\Lambda_b^0(5920)$ that they may be pentaquark states.

DOI: 10.1103/PhysRevD.104.056027

I. INTRODUCTION

Thanks to the experimental progress in the sector of heavy baryons in the past decade, many heavy baryons that cannot be ascribed to three-quark configurations have been reported [1]. For example, three narrow hidden-charm pentaquarks, namely $P_c(4312)$, $P_c(4440)$, and $P_c(4450)$, were observed by the LHCb Collaboration in the $J/\psi p$ invariant mass distributions of the $\Lambda_b \to J/\psi p K$ decay [2]. Soon afterwards, a new possible strange hidden charm pentaquark $P_{cs}(4459)$ was observed by the LHCb Collaboration with $udsc\bar{c}$ component in the $\Xi_b^- \to J/\psi \Lambda K^-$ process [3]. These findings stirred an active discussion on the structure of these states. A classical way to describe these states is treating them as candidates of meson-baryon molecular picture [4,5].

Investigating the pentaquark states has been a long history. Even before the quark model was proposed by Gell-Mann and Zweig, the $\Lambda(1405)$ had been suggested as a bound state from the $\bar{K}N$ interaction [6]. To understand the strange magnetic momentum problem and the mass inversion problem, Zou and his collaborators propose that there should exist considerable five-quark ($uuds\bar{s}$) configurations in the $N(1535)$ [7], and the five-quark components also provided a natural explanation for its large couplings to the strange $\bar{K}\Lambda$, $\bar{K}\Sigma$, $N\phi$, and $N\eta'$ channels [8–10]. By analyzing the experimental data, people suggested that $N(1875)$ and $N(2100)$ might be hidden-strangeness pentaquarks instead of a naïve three-quark state [11]. Even though, there are many "missing resonances" in this mass region that were predicted by the quark model. The detailed discussions about the pentaquark states can be found in Ref. [12].

Although people interpret some states as the pentaquark states, other possible explanations such as the three-quark state (as long as quantum numbers allow, it might well be the case) cannot be fully excluded. The possible reason is that the quark pair creation model still suffers from relatively large uncertainties [13]. Strictly speaking, these hadrons are not perfect candidates of pentaquark states. We take the state $\Xi_b(6227)$ as an example. Being considered as a traditional bottom baryon with dsb three quark component, the strong decays of this state have been studied by using the heavy quark light diquark model [14] and QCD sum rule [15]. On the other hand, many works treat $\Xi_b(6227)$ as candidates of the molecular state with $\bar{u}udsb$ five-quark component [16,17] because the mass

*20132013@cqnu.edu.cn

gap between the $\Xi_b(6227)$ and the ground Ξ_b, about 440 MeV, is large enough to excite a light quark-antiquark pair $\bar{u}u$ to form a molecular state. However, it is easy to confirm that the new P_c [$P_c(4312)$, $P_c(4440)$, and $P_c(4450)$] and $P_{cs}(4459)$ contain at least five valence quarks according to the quark components of decay model $J/\psi p$ and $J/\psi\Lambda$ [2,3]. So they are perfect candidates of hidden-charm pentaquark states.

However, in addition to finding the four hidden-charm pentaquark states in LHCb experiment [2,3], there is no significant discovery like the P_c or P_{cs} structures has been made searching in the pentaquark spectrum. Facing the present status of the experiment in detecting the pentaquarks, more studies about pentaquarks, in theory, should be considered. In fact, the hidden-charm pentaquarks P_c and P_{cs} were predicted [18–20], and suggested to be searched for in different processes [21,22]. We also note that the hidden-charm and hidden-bottom pentaquark molecular states are studied by considering different options [23,24]. In the current work, we perform a study of possible pentaquark molecular states $\Lambda_b^0(5912)$ and $\Lambda_b^0(5920)$ productions in the $\gamma p \to \Lambda_b^{0(*)} B^+$ reactions.

In 2012, two narrow excited Λ_b states, $\Lambda_b^0(5912)$ and $\Lambda_b^0(5920)$, were first observed by the LHCb Collaboration as a narrow peak in the $\Lambda_b^0\pi^+\pi^-$ invariant mass spectrum [25]. The latter state was confirmed by the CDF Collaboration [26]. Following the discovery of the $\Lambda_b^0(5912)$ and $\Lambda_b^0(5920)$, many works treated them as traditional bottom baryon [27–30]. However, the pentaquark molecular states interpretation was also supported by Refs. [31–34]. Currently, High energy photon beams are available at the Electron-Ion Collider in China (EICC) [35] or the United States (US-EIC) [36], which provide another alternative to studying $\Lambda_b^0(5912)$ and $\Lambda_b^0(5920)$. Thus, it will be helpful to understand the nature of the $\Lambda_b^0(5912)$ and $\Lambda_b^0(5920)$ if we can observe them in $\gamma p \to \Lambda_b^{0(*)} B^+$ production processes.

This paper is organized as follows. In Sec. II, we will present the theoretical formalism. In Sec. III, the numerical result of the $\gamma p \to \Lambda_b^{0(*)} B^+$ will be given, followed by discussions and conclusions in the last section.

II. THEORETICAL FORMALISM

We study the $\gamma p \to \Lambda_b^{0(*)} B^+$ reactions within the effective Lagrangian approach, which has been widely employed to investigate photoproduction processes. The tree level Feynman diagrams for the $\gamma p \to \Lambda_b^{0(*)} B^+$ reactions are depicted in Fig. 1, where the contributions from the t-channel B^- and B^{*-} exchange (a), s-channel nucleon pole (b), and contact term (c) are taken into account.

In order to compute the diagrams shown in Fig. 1, we need the effective Lagrangian densities for the relevant interaction vertices. As mentioned in the chiral unitary approach of Refs. [31–34], the $\Lambda_b^0(5912)$ and $\Lambda_b^0(5920)$ resonances are identified as s-wave meson-baryon molecules, where $\Lambda_b^0(5912)$ includes big $N\bar{B}$ and $N\bar{B}^*$ components and $\Lambda_b^0(5920)$ possesses a big $N\bar{B}^*$ component. For the $\Lambda_b^0 N\bar{B}$, $\Lambda_b^0 N\bar{B}^*$, and $\Lambda_b^{*0} N\bar{B}^*$ couplings, we can write down the Lagrangian densities as

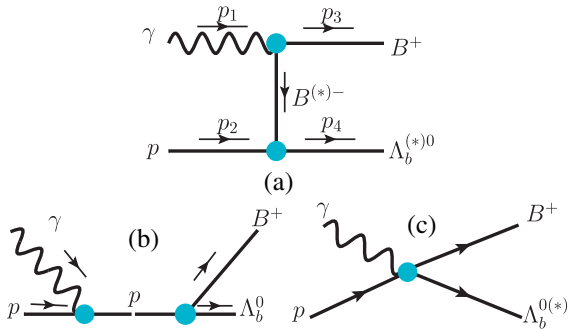

FIG. 1. Feynman diagrams for the $\gamma p \to \Lambda_b^{0(*)} B^+$ reaction. The contributions from the t-channel $B^{(*)-}$ exchange (a), s-channel nucleon pole (b), and contact term (c) are considered. In the first diagram, we also show the definition of the kinematical (p_1, p_2, p_3, p_4) that we use in the present calculation. Here, Λ_b^0 and Λ_b^{*0} refer to $\Lambda_b^0(5912)$ and $\Lambda_b^0(5920)$, respectively.

$$\mathcal{L}_{\Lambda_b^0 N\bar{B}} = g_{\Lambda_b^0 N\bar{B}} \bar{\Lambda}_b^0 N\bar{B}, \tag{1}$$

$$\mathcal{L}_{\Lambda_b^0 N\bar{B}^*} = g_{\Lambda_b^0 N\bar{B}^*} \bar{\Lambda}_b^0 \gamma^\mu N\bar{B}^*_\mu, \tag{2}$$

$$\mathcal{L}_{\Lambda_b^{0*} N\bar{B}^*} = g_{\Lambda_b^{*0} N\bar{B}^*} \bar{\Lambda}_b^{*0\mu} N\bar{B}^*_\mu. \tag{3}$$

The coupling constants in the above Lagrangians were determined in Ref. [34] in a hadronic molecular picture with $g_{\Lambda_b^0 N\bar{B}} = 4.6$, $g_{\Lambda_b^0 N\bar{B}^*} = 3.0$, and $g_{\Lambda_b^{*0} N\bar{B}^*} = 5.7$.

To compute the amplitudes of the diagrams shown in Fig. 1, the effective Lagrangian densities related to the photon which are required [37]

$$\mathcal{L}_{\gamma pp} = -e\bar{p}\left(\gamma^\mu - \frac{\kappa_p}{2m_p}\sigma^{\mu\nu}\partial_\nu\right)A^\mu p, \tag{4}$$

$$\mathcal{L}_{\gamma B^*\bar{B}} = \frac{g_\gamma B^{*+} B^+}{4} e\epsilon^{\mu\nu\alpha\beta} F_{\mu\nu} B^{*+}_{\alpha\beta} B^- + \frac{g_\gamma B^{*0} B^0}{4} e\epsilon^{\mu\nu\alpha\beta} F_{\mu\nu} B^{*0}_{\alpha\beta} \bar{B}^0 + \text{H.c.}, \tag{5}$$

$$\mathcal{L}_{\gamma B^- B^+} = ieA_\mu (B^- \partial^\mu B^+ - B^+ \partial^\mu B^-), \tag{6}$$

where the strength tensor is defined as $\sigma^{\mu\nu} = \frac{i}{2}(\gamma^\mu\gamma^\nu - \gamma^\nu\gamma^\mu)$, $F_{\mu\nu} = \partial_\mu A_\nu - \partial_\nu A_\mu$, and $B^*_{\alpha\beta} = \partial_\alpha B^*_\beta - \partial_\beta \bar{B}^*_\alpha$. The anomalous magnetic momentum $\kappa_p = 1.79$ and the $\alpha = e^2/4\pi = 1/137$ is the electromagnetic fine structure constant. The coupling constant $g_{\gamma B^{*+} B^+}$ and $g_{\gamma B^{*0} B^0}$ are determined from

the partial decay width of $B^{*+} \to B^+\gamma$ and $B^{*0} \to B^0\gamma$, which is obtained from Eq. (5),

$$\Gamma(B^{*+} \to B^+\gamma) = \frac{\alpha g^2_{\gamma B^{*+}B^+}}{24} m_{B^{*+}}(m^2_{B^{*+}} - m^2_{B^+}), \quad (7)$$

$$\Gamma(B^{*0} \to B^0\gamma) = \frac{\alpha g^2_{\gamma B^{*0}B^0}}{24} m_{B^{*0}}(m^2_{B^{*0}} - m^2_{B^0}), \quad (8)$$

where m_{B^*} and m_B are the mass of B^* and B, respectively. However, the width of the B^* meson is not well determined experimentally. In the present work, we use the theoretical predicted partial widths in Ref. [38] and the coupling constants are determined to be $g_{\gamma B^{*+}B^+} = 1.308\ \text{GeV}^{-1}$ and $g_{\gamma B^{*0}B^0} = -0.745\ \text{GeV}^{-1}$.

In evaluating the scattering amplitudes of the $\gamma p \to \Lambda_b^{0(*)} B^+$ reactions, we need to include the form factors because hadrons are not pointlike particles. For the t-channel B and B^* mesons exchange, we would like to apply a widely used pole form factor, which is

$$\mathcal{F}_i = \frac{\Lambda_i^2 - m_i^2}{\Lambda_i^2 - q_i^2}, \qquad i = B, B^*, \quad (9)$$

where $\Lambda_i = m_i + \alpha\Lambda_{\text{QCD}}$ and the QCD energy scale $\Lambda_{\text{QCD}} = 220$ MeV. The parameter α reflects the nonperturbative property of QCD at the low-energy scale, which will be taken as a parameter and discussed later. For the s-channel nucleon pole process, we adopt a form factor

$$\mathcal{F}_N(q^2, m_N^2) = \frac{\Lambda_N^4}{\Lambda_N^4 + (q^2 - m_N^2)^2}, \quad (10)$$

with $\Lambda_N = 0.9$ GeV, which can be well used to reproduce experimental data of some reactions [39,40].

With the above effective Lagrangian densities, the scattering amplitudes for the $\gamma p \to \Lambda_b^0(5912)B^+$ and $\gamma p \to \Lambda_b^0(5920)B^+$ reactions can be obtained straightforwardly. First, we write the scattering amplitudes for the $\gamma p \to \Lambda_b^0(5912)B^+$ reaction

$$\mathcal{M}_t^B = -ieg_{\Lambda_b^0 N\bar{B}}\bar{u}_{\Lambda_b^0}(p_4, s_4)u_p(p_2, s_2)\frac{1}{q_t^2 - m_{\bar{B}}^2}(p_3^\mu - q_t^\mu) \times \epsilon_\mu(p_1, s_1)\mathcal{F}_B, \quad (11)$$

$$\mathcal{M}_t^{B^*} = i\frac{eg_{\Lambda_b^0 N\bar{B}^*}g_{\gamma B^{*+}B^+}}{4}\epsilon^{\rho\eta\alpha\beta}(p_{1\rho}g_{\eta\lambda} - p_{1\eta}g_{\rho\lambda}) \times (q_{t\alpha}g_{\beta\sigma} - q_{t\beta}g_{\alpha\sigma})\epsilon^\lambda(p_1, s_1)\frac{-g^{\mu\sigma} + q_t^\mu q_t^\sigma/m_{\bar{B}^*}^2}{q_t^2 - m_{\bar{B}^*}^2} \times \bar{u}_{\Lambda_b^0}(p_4, s_4)\gamma_\mu u_p(p_2, s_2)\mathcal{F}_{B^*}, \quad (12)$$

$$\mathcal{M}_s^N = -ieg_{\Lambda_b^0 N\bar{B}}\bar{u}_{\Lambda_b^0}(p_4, s_4)\frac{\not{q}_s + m_p}{q_s^2 - m_p^2} \times \left[\gamma^\mu + \frac{\kappa_p}{4m_p}(\gamma^\mu \not{p}_1 - \not{p}_1\gamma^\mu)\right] \times u_p(p_2, s_2)\epsilon_\mu(p_1, s_1)\mathcal{F}_N. \quad (13)$$

Then the amplitudes for the $\gamma p \to \Lambda_b^0(5920)B^+$ reaction have the form

$$\mathcal{M}_{t2}^{B^*} = i\frac{eg_{\Lambda_b^{*0} N\bar{B}^*}g_{\gamma B^{*+}B^+}}{4}\epsilon^{\rho\lambda\alpha\beta}(p_{1\rho}g_{\lambda\eta} - p_{1\lambda}g_{\rho\eta}) \times (q_{t\alpha}g_{\beta\nu} - q_{t\beta}g_{\alpha\nu})\epsilon^\eta(p_1, s_1)\frac{-g^{\mu\nu} + q_t^\mu q_t^\nu/m_{\bar{B}^*}^2}{q_t^2 - m_{\bar{B}^*}^2} \times \bar{u}^\mu_{\Lambda_b^{*0}}(p_4, s_4)u_p(p_2, s_2)\mathcal{F}_{B^*}. \quad (14)$$

In the above equations, the $q_s = p_1 + p_2 = p_3 + p_4$ and $q_t = p_1 - p_3 = p_4 - p_2$.

The contact term illustrated in Fig. 1(c) serves to keep the full amplitude gauge invariant. For the present calculation, we adopt the following form

$$\mathcal{M}^c_{\gamma p \to \Lambda_b^0(5912)B^+} = ieg_{\Lambda_b^0 N\bar{B}}\bar{u}_{\Lambda_b^0}(p_4, s_4)[\mathcal{A}(\gamma^\mu - 1) + \mathcal{B}] \times u_p(p_2, s_2)\epsilon^\mu(p_1, s_1), \quad (15)$$

$$\mathcal{M}^c_{\gamma p \to \Lambda_b^0(5920)B^+} = 0, \quad (16)$$

with

$$\mathcal{A} = \frac{-m_p\mathcal{F}_N}{(q_s^2 - m_p^2)}, \qquad \mathcal{B} = \frac{\mathcal{F}_B}{(q_t^2 - m_{\bar{B}}^2)}2p_3^\mu + \frac{\mathcal{F}_N}{q_s^2 - m_p^2}2p_2^\mu. \quad (17)$$

The differential cross section in the c.m. frame for the $\gamma p \to \Lambda_b^0(5912)B^+$ and $\gamma p \to \Lambda_b^0(5920)B^+$ reactions are calculated using the following equation:

$$\frac{d\sigma}{d\cos\theta} = \frac{m_N m_{\Lambda_b^{0(*)}}}{32\pi q_s^2}\frac{|\vec{p}_3^{\,c.m}|}{|\vec{p}_1^{\,c.m}|}\sum_{s_1,s_2,s_3,s_4}|\mathcal{M}_{1,2}|^2, \quad (18)$$

where $\mathcal{M}_1 = \mathcal{M}_t^B + \mathcal{M}_t^{B^*} + \mathcal{M}_s^N + \mathcal{M}^c_{\gamma p \to \Lambda_b^0(5912)B^+}$ and $\mathcal{M}_2 = \mathcal{M}_{t2}^{B^*}$ are total scattering amplitude of the $\gamma p \to \Lambda_b^0(5912)B^+$ and $\gamma p \to \Lambda_b^0(5920)B^+$ reactions, respectively. The θ is the scattering angle of the outgoing B^+ meson relative to the beam direction, while $\vec{p}_1^{\,c.m}$ and $\vec{p}_3^{\,c.m}$ are the photon and B^+ meson three momenta in the c.m. frame, respectively, which are

$$|\vec{p}_1^{\,c.m}| = \frac{\lambda^{1/2}(q_s^2, 0, m_N^2)}{2\sqrt{q_s^2}}, \quad |\vec{p}_3^{\,c.m}| = \frac{\lambda^{1/2}(q_s^2, m_{B^+}^2, m_{\Lambda_B^{0(*)}}^2)}{2\sqrt{q_s^2}}, \tag{19}$$

where the λ is the Källen function with $\lambda(x, y, z) = (x - y - z)^2 - 4yz$.

III. RESULTS

Considering the $\Lambda_b^0(5912)$ and $\Lambda_b^0(5920)$ as pentaquark molecule, their production in the $\gamma p \to \Lambda_b^0(5912)B^+$ and $\gamma p \to \Lambda_b^0(5920)B^+$ reactions are evaluated. The mechanism including the t channel mediated by the exchange of $\bar{B}^*$ mesons, the contact term, and the s channel where nucleon is considered as an intermediate state. To make a reliable prediction for the cross section of the $\gamma p \to \Lambda_b^0(5912)B^+$ and $\gamma p \to \Lambda_b^0(5920)B^+$ reactions, the only issue we need to clarify is the explicit form of the parameter α relation to the form factors. The parameter α reflects the nonperturbative property of QCD at the low-energy scale and could not be determined by the first principles. It is usually determined from the experimental branching ratios. Next, how to compute the value of α is shown in detail.

With the formalism and ingredients give in Sec. II, the total cross section of $\gamma p \to \Lambda_b^0(5912)B^+$ and $\gamma p \to \Lambda_b^0(5920)B^+$ reactions versus the model parameter α are computed. The results obtained with several c.m. energy W are shown in Fig. 2. We find that the value of the cross section increases continuously but relatively slowly with the increasing of α and in particular, taking $W = 12$ GeV as an example, and varying the cutoff parameter from 0.0 to 5.0, the value of the cross section runs from nearly 0.0 to 0.2 nb and is not very sensitive to the model parameter α compared with the cross section with larger α. This result is consistent with the findings in Refs. [37,41–44] that α is restricted within a reasonable range from 0.0 to 5.0 by the experimental data.

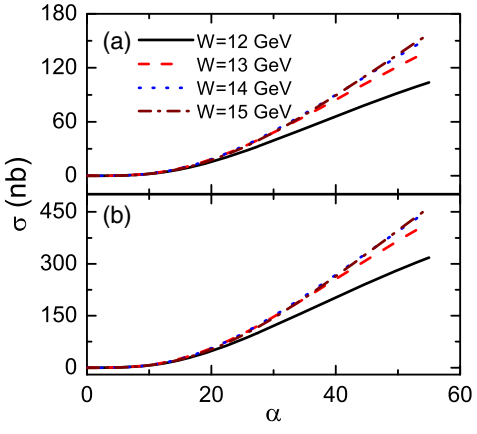

FIG. 2. Cross section of the $\gamma p \to \Lambda_b^0(5912)B^+$ (a) and the $\gamma p \to \Lambda_b^0(5920)B^+$ (b) with different energy in the c.m. frame depending on the parameter α.

Once the model parameter α is determined, the total cross sections versus the c.m. energy W of the γp system for $\gamma p \to \Lambda_b^0(5912)B^+$ and $\gamma p \to \Lambda_b^0(5920)B^+$ reactions can be evaluated. In Fig. 3, the total cross section of the $\gamma p \to \Lambda_b^0(5912)B^+$ and $\gamma p \to \Lambda_b^0(5920)B^+$ reactions with different α are presented, where we restrict the α value within a reasonable range from 1.0 to 2.0. It is worth mentioning that the value of the cross section is very sensitive to the α. To see how much it depends on the cutoff parameter, we take the cross section at an energy about W = 12 GeV with the range of $\alpha = 1.0$–2.0 as example. The so-obtained cross section ranges from 4.5×10^{-4} nb to 6.6×10^{-3} nb for the $\gamma p \to \Lambda_b^0(5912)B^+$ reaction and 1.4×10^{-3} nb to 2.1×10^{-2} nb for the $\gamma p \to \Lambda_b^0(5920)B^+$ reaction. It would be then convenient to narrow the range of the alpha parameter.

Fortunately, more stringent constraints for the α value have been made by comparing with the experimental data [44,45]. As the free parameter in our calculation, $\alpha = 1.38$ or 1.81 is fixed by fitting the experimental data of Ref. [45], whose procedures are just illustrated in Ref. [44]. In this work, we adopt the parameter $\alpha = 1.38$ or 1.81 because this value is determined from the experimental data of Ref. [45] within the same B and B^* form factors adopted in the current work of Ref. [44]. The results for the c.m. energy W from the reaction threshold to 15.0 GeV are shown in Fig. 4.

From the Fig. 4, one can see that the total cross section increases sharply near the threshold. At higher energies, the cross section increases continuously but relatively slowly compared with that near threshold. However, the total cross section decreases, but very slowly, when we change the c.m. energy W form 13.6 to 15.0 GeV. The results also show that the total cross section with $\alpha = 1.81$ is bigger than that of $\alpha = 1.38$. The difference between the cross section predicted with $\alpha = 1.38$ and that predicted with $\alpha = 1.83$ becomes larger with the energy increasing.

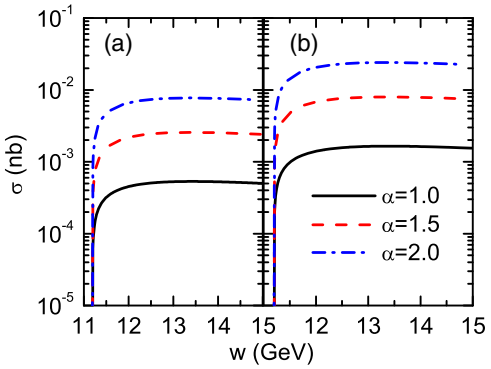

FIG. 3. The total cross section for the processes (a) $\gamma p \to \Lambda_b^0(5912)B^+$ and (b) $\gamma p \to \Lambda_b^0(5920)B^+$ with different α.

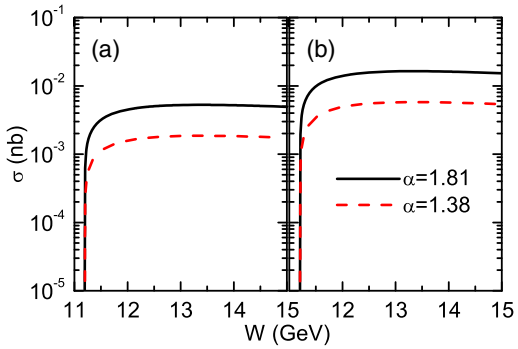

FIG. 4. The total cross section for the processes (a) $\gamma p \to \Lambda_b^0(5912)B^+$ and (b) $\gamma p \to \Lambda_b^0(5920)B^+$ with different α.

The results show that the total cross section for $\Lambda_b^0(5920)$ production is bigger than that for $\Lambda_b^0(5912)$ production. At a c.m. energy of about 13.6 GeV and a parameter $\alpha = 1.81$ ($\alpha = 1.38$), the cross section is of the order of 0.0164 (0.0057) nb for $\Lambda_b^0(5920)$ production and 0.00527 (0.00186) nb for $\Lambda_b^0(5912)$ production, which is very challenging to search for them at EICC [35] but possible at US-EIC [36] due to a higher luminosity. If the luminosity of EICC increases at least one order of magnitude, these states would be hopefully detected in photoproduction reaction.

We also find that the line shapes of the cross section between the $\gamma p \to \Lambda_b^0(5912)B^+$ reaction and the $\gamma p \to \Lambda_b^0(5920)B^+$ reaction are the same. A possible explanation for this may be that the t-channel B^* meson exchange plays a predominant role in these two reactions. And this is guessed from the $\Lambda_b^0(5920)$ production mechanism including only the t-channel $\bar{B}^*$ meson exchange. We indeed find from Fig. 5 that the individual contributions of the t-channel $\bar{B}^*$ meson exchange play a dominant role in the $\gamma p \to \Lambda_b^0(5912)B^+$ reaction, while the contributions from the t-channel $\bar{B}$ meson exchange, s-channel nucleon pole and contact term are small. Moreover, the interferences among them are quite small, which makes that the t-channel $\bar{B}^*$ meson exchange contribution almost saturates the total cross section. The dominant $\bar{B}^*$ meson exchange contribution can be easily understood since the $\Lambda_b^0(5912)$ and $\Lambda_b^0(5920)$ resonances are assumed as the molecular state with a big $\bar{B}^*N$ component [31–34].

Our calculation indicates that the contributions from the s-channel nucleon pole is quite small, and the value is about of the order of 10^{-6} nb. A possible explanation for this may be that the nucleon is so far off the threshold. It naturally leads us to think about whether there are contributions that come from nucleon excited states or other baryonic states, which can enhance the cross section of $\gamma p \to \Lambda_b^0(5912)B^+$, and $\gamma p \to \Lambda_b^0(5920)B^+$ reactions make the EICC easily detect the current luminosity design. Unfortunately, there is no information on these studies. Thus, we do not consider the contributions from other states with heavier mass in this work.

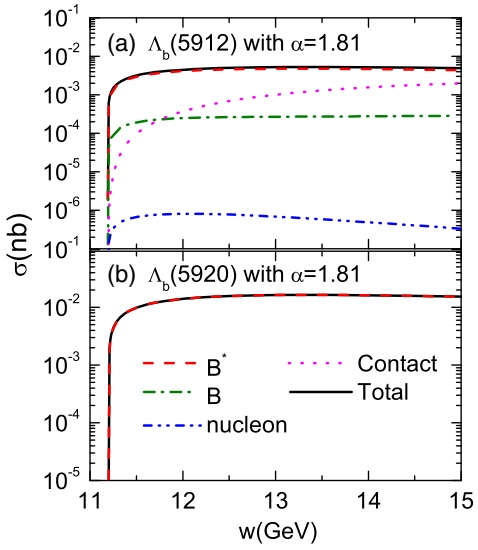

FIG. 5. Individual contributions of the t-channel B (dash dot line) and B^* (red dash line) exchange, s-channel nucleon pole (dash dot dot line), and contact term (dot line) for the processes $\gamma p \to \Lambda_b^0(5912)B^+$ and $\gamma p \to \Lambda_b^0(5920)B^+$ as a function of the energy.

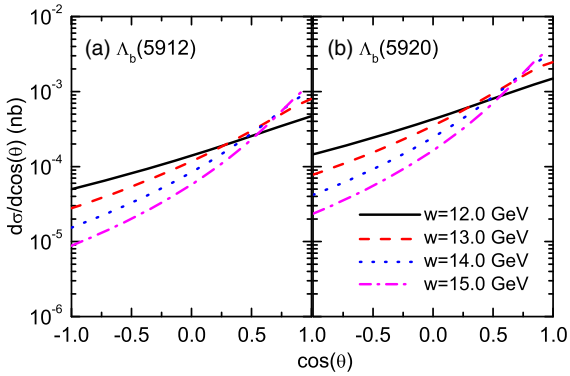

FIG. 6. (a) The $\gamma p \to \Lambda_b^0(5912)B^+$ and (b) $\gamma p \to \Lambda_b^0(5920)B^+$ differential cross sections at different energies with $\alpha = 1.81$. The black solid lines, red dashed lines, blue dotted lines, and straight dashed-dotted lines are obtained at c.m. energies $W = 12.0$, 13.0, 14.0, and 15.0 GeV, respectively.

In addition to the total cross section, we also compute the differential cross section for the $\gamma p \to \Lambda_b^0(5912)B^+$ and $\gamma p \to \Lambda_b^0(5920)B^+$ reactions as a function of the scattering angle of the outgoing meson relative to the beam direction at different c.m. energies, i.e., $W = 12.0$, 13.0, 14.0, and 15.0 GeV. The theoretical results are shown in Fig. 6. We note that the differential cross section is largest at the extreme forward angle and decreases with the increase of the scattering angle. This is because the t-channel $\bar{B}^*$ meson exchange plays a predominant role in the $\gamma p \to \Lambda_b^0(5912)B^+$ and $\gamma p \to \Lambda_b^0(5920)B^+$ reactions.

IV. SUMMARY

Stimulated by the newly observed pentaquark spectrum like P_c or P_{cs} structure, pentaquark spectroscopy containing bottom quark is emerging. In 2012, the $\Lambda_b^0(5912)$ and $\Lambda_b^0(5920)$ were first observed by the LHCb Collaboration as narrow peak in the $\Lambda_b^0\pi^+\pi^-$ invariant mass spectrum [25]. Many works treat them as pentaquark molecular states [31–34] with a $\bar{B}^*N$ component for $\Lambda_b^0(5920)$ and $\bar{B}^{(*)}N$ components for $\Lambda_b^0(5912)$. And they cannot be detected like P_c or P_{cs} through a heavy hadron decay to $\bar{B}^{(*)}N$ plus a light meson, since their masses are just below the $\bar{B}^{(*)}N$ threshold.

In this paper, we made a detailed exploration of the nonresonant contribution to the $\gamma p \to \Lambda_b^0(5912)B^+$ and $\gamma p \to \Lambda_b^0(5920)B^+$, with the aim to find a reasonable estimation of the $\Lambda_b^0(5912)$ and $\Lambda_b^0(5920)$ production rates at relatively high energies, where no data are available at this point. The production process is described by the t-channel $\bar{B}^{(*)-}$ exchange, s-channel nucleon pole, and contact term. The coupling constants of the $\Lambda_b^0(5912)$ to $\bar{B}^{(*)}N$ and $\Lambda_b^0(5920)$ to $\bar{B}^*N$ are obtained from chiral unitary theory [31–34], where $\Lambda_b^0(5912)$ and $\Lambda_b^0(5920)$ are dynamically generated.

Our calculation indicates that the cross section for $\gamma p \to \Lambda_b^0(5912)B^+$ and $\gamma p \to \Lambda_b^0(5920)B^+$ reactions can reach 0.0164 nb and 0.00527 nb, respectively, are too small to be observed due to out of reach of the current luminosity design $(2–4) \times 10^{33}\ \mathrm{cm}^{-2}\,\mathrm{s}^{-1}$ of the EICC [35]. If the luminosity of the EICC increases at least one order of magnitude, these states would be hopefully detected in photoproduction reaction. For the proposed US-EIC with the luminosity of $10^{34}\ \mathrm{cm}^{-2}\,\mathrm{s}^{-1}$ or higher, it would be possible to observe these states [36]. Moreover, the differential cross sections computed also can be used to test the molecular picture of the $\Lambda_b^0(5912)$ and $\Lambda_b^0(5920)$.

ACKNOWLEDGMENTS

This work was supported by the Science and Technology Research Program of Chongqing Municipal Education Commission (Grant No. KJQN201800510), the Opened Fund of the State Key Laboratory on Integrated Optoelectronics (Grant No. IOSKL2017KF19). Yin Huang want to thanks the support from the Development and Exchange Platform for the Theoretic Physics of Southwest Jiaotong University under Grants No. 11947404 and No. 12047576, the Fundamental Research Funds for the Central Universities (Grant No. 2682020CX70), and the National Natural Science Foundation of China under Grant No. 12005177.

[1] P. A. Zyla *et al.* (Particle Data Group), Prog. Theor. Exp. Phys. (**2020**), 083C01.
[2] R. Aaij *et al.* (LHCb Collaboration), Phys. Rev. Lett. **122**, 222001 (2019).
[3] R. Aaij *et al.* (LHCb Collaboration), Sci. Bull. **66**, 1278 (2021).
[4] H. X. Chen, W. Chen, X. Liu, and X. H. Liu, Eur. Phys. J. C **81**, 409 (2021).
[5] R. Chen, Eur. Phys. J. C **81**, 122 (2021).
[6] R. H. Dalitz and S. F. Tuan, Phys. Rev. Lett. **2**, 425 (1959).
[7] B. S. Zou, Nucl. Phys. **A835**, 199 (2010).
[8] B. C. Liu and B. S. Zou, Phys. Rev. Lett. **96**, 042002 (2006).
[9] M. Doring, E. Oset, and B. S. Zou, Phys. Rev. C **78**, 025207 (2008).
[10] C. S. An and B. S. Zou, Eur. Phys. J. A **39**, 195 (2009).
[11] J. He, Phys. Rev. D **95**, 074031 (2017).
[12] F. K. Guo, C. Hanhart, U. G. Meiner, Q. Wang, Q. Zhao, and B. S. Zou, Rev. Mod. Phys. **90**, 015004 (2018).
[13] X. Liu, Z. G. Luo, and Z. F. Sun, Phys. Rev. Lett. **104**, 122001 (2010).
[14] B. Chen, K. W. Wei, X. Liu, and A. Zhang, Phys. Rev. D **98**, 031502 (2018).
[15] K. Azizi, Y. Sarac, and H. Sundu, J. High Energy Phys. 03 (2021) 244.
[16] Y. Huang, C. j. Xiao, L. S. Geng, and J. He, Phys. Rev. D **99**, 014008 (2019).
[17] Q. X. Yu, R. Pavao, V. R. Debastiani, and E. Oset, Eur. Phys. J. C **79**, 167 (2019).
[18] J. J. Wu, R. Molina, E. Oset, and B. S. Zou, Phys. Rev. C **84**, 015202 (2011).
[19] J. X. Lu, E. Wang, J. J. Xie, L. S. Geng, and E. Oset, Phys. Rev. D **93**, 094009 (2016).
[20] V. V. Anisovich, M. A. Matveev, J. Nyiri, A. V. Sarantsev, and A. N. Semenova, Int. J. Mod. Phys. A **30**, 1550190 (2015).
[21] Y. Huang, J. He, H. F. Zhang, and X. R. Chen, J. Phys. G **41**, 115004 (2014).
[22] A. Feijoo, V. K. Magas, A. Ramos, and E. Oset, Eur. Phys. J. C **76**, 446 (2016).
[23] F. L. Wang, R. Chen, and X. Liu, Phys. Rev. D **103**, 034014 (2021).
[24] J. T. Zhu, S. Y. Kong, Y. Liu, and J. He, Eur. Phys. J. C **80**, 1016 (2020).
[25] R. Aaij *et al.* (LHCb Collaboration), Phys. Rev. Lett. **109**, 172003 (2012).

[26] T. A. Aaltonen *et al.* (CDF Collaboration), Phys. Rev. D **88**, 071101 (2013).
[27] K. L. Wang, Y. X. Yao, X. H. Zhong, and Q. Zhao, Phys. Rev. D **96**, 116016 (2017).
[28] K. Gandhi, A. Kakadiya, Z. Shah, and A. K. Rai, AIP Conf. Proc. **2220**, 140015 (2020).
[29] Y. Kawakami and M. Harada, Phys. Rev. D **99**, 094016 (2019).
[30] Y. Kawakami and M. Harada, Phys. Rev. D **97**, 114024 (2018).
[31] O. Romanets, C. Garcia-Recio, L. L. Salcedo, J. Nieves, and L. Tolos, Acta Phys. Pol. B Proc. Suppl. **6**, 973 (2013).
[32] J. X. Lu, Y. Zhou, H. X. Chen, J. J. Xie, and L. S. Geng, Phys. Rev. D **92**, 014036 (2015).
[33] W. H. Liang, C. W. Xiao, and E. Oset, Phys. Rev. D **89**, 054023 (2014).
[34] C. Garcia-Recio, J. Nieves, O. Romanets, L. L. Salcedo, and L. Tolos, Phys. Rev. D **87**, 034032 (2013).
[35] D. P. Anderle, V. Bertone, X. Cao, L. Chang, N. Chang, G. Chen, X. Chen, Z. Chen, Z. Cui, L. Dai *et al.*, Front. Phys. (Beijing) **16**, 64701 (2021).
[36] A. Accardi, J. L. Albacete, M. Anselmino, N. Armesto, E. C. Aschenauer, A. Bacchetta, D. Boer, W. K. Brooks, T. Burton, N. B. Chang *et al.*, Eur. Phys. J. A **52**, 268 (2016).
[37] C. J. Xiao and D. Y. Chen, Phys. Rev. D **96**, 014035 (2017).
[38] H. M. Choi, Phys. Rev. D **75**, 073016 (2007).
[39] S. H. Kim, S. i. Nam, Y. Oh, and H. C. Kim, Phys. Rev. D **84**, 114023 (2011).
[40] Y. Oh, K. Nakayama, and T.-S. H. Lee, Phys. Rep. **423**, 49 (2006).
[41] Y. Dong, A. Faessler, T. Gutsche, Q. Lü, and V. E. Lyubovitskij, Phys. Rev. D **96**, 074027 (2017).
[42] D. Y. Chen, X. Liu, and T. Matsuki, Phys. Rev. D **87**, 054006 (2013).
[43] G. Li, F. l. Shao, C. W. Zhao, and Q. Zhao, Phys. Rev. D **87**, 034020 (2013).
[44] P. Colangelo, F. De Fazio, and T. N. Pham, Phys. Lett. B **542**, 71 (2002).
[45] I. Adachi *et al.* (Belle Collaboration), arXiv:1209.6450.